

# OBSERVATIONAL INVESTIGATION OF THE LOW-LEVEL JETS IN THE METROPOLITAN REGION OF SÃO PAULO, BRAZIL

*Maciel Piñero Sanches<sup>1</sup>, Amauri Pereira de Oliveira<sup>1</sup>, Janet Valdés Tito<sup>1</sup>, Ramón Pérez Varona<sup>2</sup>, Georgia Codato<sup>1</sup>, Flavia Noronha Dutra Ribeiro<sup>3</sup>, Edson Pereira Marques Filho<sup>4</sup>, Lucas Cardoso da Silveira<sup>1</sup>*

<sup>1</sup> Department of Atmospheric Sciences, Institute of Astronomy, Geophysics and Atmospheric Sciences, University of São Paulo, São Paulo, Brazil ([maciel.pinero@iag.usp.br](mailto:maciel.pinero@iag.usp.br), [apdolive@usp.br](mailto:apdolive@usp.br), [janet.valdes@iag.usp.br](mailto:janet.valdes@iag.usp.br), [gecodato@usp.br](mailto:gecodato@usp.br), [lucas.silveira@usp.br](mailto:lucas.silveira@usp.br))

<sup>2</sup> Department of Experimental Physics, Institute of Physics, University of São Paulo, São Paulo, Brazil ([rvarona90@gmail.com](mailto:rvarona90@gmail.com))

<sup>3</sup> School of Arts, Sciences and Humanities, University of São Paulo, São Paulo, Brazil ([flaviaribeiro@usp.br](mailto:flaviaribeiro@usp.br))

<sup>4</sup> Interdisciplinary Center for Energy and Environment, Federal University of Bahia, Salvador, Brazil ([edson.marques@ufba.br](mailto:edson.marques@ufba.br))

## Abstract

In this work the main features and evolution of Low-Level Jets (LLJs) in the metropolitan region of São Paulo, Brazil, are investigated using two sets of radio soundings carried out: (a) every three hours and during 10 consecutive days in the summer and winter field campaigns of the MCITY BRAZIL Project and (b) regularly two per day between 2009 and 2013. Visual inspections of wind speed and wind direction profiles indicate the presence of LLJs in 85 % of days, predominantly at nighttime during undisturbed conditions, with mean intensity and height of  $8.4 \pm 0.32 \text{ m s}^{-1}$  and  $541 \pm 26 \text{ m}$ , respectively. The predominant wind directions at the maximum wind speed level are from east, north and northeast during field campaigns of 2013. Most of the LLJs observed during both field campaigns (76 %) are associated to the inertial oscillation mechanism and modulated by the baroclinicity induced by mesoscale features of topography and land-ocean thermal contrast. The remaining cases are associated to synoptic disturbances baroclinicity. The monthly variations of LLJs properties between 2009 and 2013 were estimated using an objective method and the results showed that the LLJs are very frequent throughout the year, exceeding 65 % of days in all months. The maximum LLJs occurrence was observed in October (86 % of days) and the minimum frequency occurs in July (69 % of days). The impact of LLJs in the intensity of urban heat island and surface inversion layer was assessed during field campaign of August, 2013 and the results indicate that the shear generated by the LLJs plays an important role in reducing the SI layer and urban heat island intensity.

## 1. Introduction

During nighttime is common to observe a relative maximum in the vertical profile of wind speed at the top of the Surface Inversion (SI) layer (Blackadar, 1957; Stull, 1988). Known as Low-Level Jet (LLJ), it is defined as a relative maximum in the wind speed profile that occurs with more frequency between 100 and 500 m (Stull, 1988; Baas et al., 2009). LLJs are frequently observed during clear sky conditions and at nighttime over land characterized by homogeneous land use and flat topography. Under these conditions the progressive radiational cooling of the surface intensifies the SI, reducing friction and, as consequence, the flow above of the SI layer speeds up as it decouples from the surface, generating a maximum relative in the vertical profile of wind speed near to the surface (Stull, 1988; Baas et al., 2009; Van de Wiel et al., 2010; Wei et al., 2013; Barlow, 2014). In this case the LLJ is produced by the inertial oscillation and it can be identified by the counterclockwise rotation (Southern Hemisphere) of the ageostrophic component of the horizontal wind with Coriolis frequency  $f$  ( $f=2\Omega\sin\phi$ , where

$\Omega$  is the Earth's rotation rate and  $\phi$  is the local latitude). For the latitude of São Paulo (23.5 °S) the inertial frequency corresponds to a period of 30.5 hours.

The intensity and position of the LLJs are linked to the vertical distribution of the ageostrophic wind component, which in turn may vary according to baroclinicity induced by soil moisture distribution, land use and topographic effects, and to the turbulence intensity in the previous daytime convective boundary layer (Stull, 1988; Karam, 2002; Klein et al., 2016). First proposed by Blackadar (1957), the inertial oscillation has been used to explain LLJs by linking its nocturnal evolution to the stable and convective boundary layer (Karam, 2002; Karipot et al., 2009; Van de Wiel et al., 2010).

According to Lundquist (2003) and Kallistratova and Kouznetsov (2012), LLJs due to inertial oscillation are not as frequent as though initially. Indeed, the observations indicate that LLJs are more frequently associated to baroclinicity induced by: (a) land-ocean differential surface heating in coastal regions (Parish, 2000; Kutsher et al., 2012; Wei et al., 2013); (b) synoptic scale systems (cold fronts) (Whiteman et al., 1997); (c) differential heating in the presence of sloping terrain (Holton, 1967; Whiteman et al., 1997). LLJs can also be caused by topographical effects of mechanical origin, such as blockages of mountain barriers and channeling along valleys (Parish, 1982; Li and Chen, 1998).

The LLJs has been observed in different parts of the world, more frequently at Great Plains, USA (Song et al. 2005; Wang et al. 2007; Du et al. 2014; Klein et al. 2016; Shapiro et al. 2016; Parish, 2017); east and west of the Andes (Marengo et al., 2004; Jones, 2019; Montini et al., 2019); east, south and southwestern of China (Wei et al., 2013; Du et al., 2014; Li et al., 2018; Zhang et al., 2019); Central Western Mexico (Arfeuille et al., 2015); Cabauw, Netherlands (Baas et al., 2009); Antarctica (King et al., 2008); Negev desert of Israel (Kutsher et al., 2012) and southern Brazil (Karam, 2002; Montini et al., 2019). Knowing LLJ properties is important for planning aviation safety procedure in airports, assessing potential of wind energy production, predicting the transport of atmospheric pollutants and it can influence the development and trajectory of convective systems. Understanding LLJs behavior is particularly important over urban areas where they can increase the vertical transport of pollutants, mainly O<sub>3</sub> (Hu et al. 2013b; Klein et al. 2014; Sullivan et al. 2017) and interact with Urban Heat Island (UHI) (Kallistratova and Kouznetsov 2012; Hu et al. 2013a). Despite the increase in LLJs studies in recent years due to the development of ground-based remote sensing techniques, only a few have been done on urban areas, such as, in Moscow, Russia (Kallistratova et al., 2009; Kallistratova and Kouznetsov, 2012), Oklahoma City, USA (Wang et al. 2007; Hu et al. 2013a), London, UK (Barlow et al., 2015) and Beijing and Guangzhou, China (Miao et al., 2018). These studies concluded that LLJs over urban area are higher, weaker and occur less frequently than over rural sites and attributes the differences to the higher roughness and different thermal properties of the urban surface.

There are not observational studies of LLJs in the metropolitan region of São Paulo (MRSP) available in the literature. Some of the characteristics of these LLJs have already been investigated by Karam (2002) using tethered balloon observations in Iperó, a countryside rural area located 80 km west of the MRSP. According to Karam (2002), LLJs in this region has intensity between 8 and 10 m s<sup>-1</sup> and height around 350 m above the surface during clear-sky nights. Numerical results obtained by Karam (2002) indicate that the LLJs observed in Iperó are a result of the combination of four factors: the anabatic and katabatic circulation in the “Paulista” sector of the “Paraná” River Valley, the inertial oscillation and the sea-breeze circulation. This hypothesis will be investigated as a possible explanation for the LLJs observed in the MRSP.

The objective of this work is to investigate the main features of the LLJs observed in the MRSP, such as frequency of occurrence, speed, height and direction. Diurnal and seasonal variation and mechanisms of LLJ formation are also investigated. The analysis will be made from the radio soundings carried out every 3-hour during the two 10-days field campaigns of the MCITY BRAZIL Project in February and August of 2013 (Oliveira et al. 2019). This characterization is complemented using radio soundings carried out regularly twice a day over four years at the “Campo de Marte” Airport (ACM) of São Paulo City.

## 2. Materials and methods

### 2.1. Region of study

The MRSP is located in the southeastern Brazil on the “Paulista” plateau at 722 m above sea level (asl) and 65 km from the Atlantic Ocean. It is composed of 39 municipalities in the form of conurbation (Fig. 1a), with a population of approximately 21.7 million habitants (IBGE, 2018). Figure 1b, c shows the complex topography of the MRSP, which can be represented by a cross dashed yellow line oriented from northwest to southeast direction. From Atlantic Ocean to the continent, it is observed several elevations that form part of the “Serra do Mar” (200-750 m asl), followed by the “Paulista” plateau. The urban area of the MRSP is located in the “Paulista” plateau (Fig. 1c), limited at the north and northwest by a chain of three ridges (“Tiete”, “Tamanduati” and “Pinheiros”) varying from 300 to 700 m asl (Fig. 1b).

The climate characterization of MRSP is based on monthly mean values obtained between 1960-1990 on the meteorological surface station of MIRANTE (23°29'47"S, 46°37'11"W, 792 m asl) (Fig. 1a). According the Köppen classification of Alvares et al. (2014), the climate of MRSP is typical of subtropical regions and can be classified as high elevation subtropical humid (Cwb), with a dry and cold winter during June-August and a wet and warm summer during December-March (Oliveira et al., 2003). The monthly mean minimum of air temperature and specific humidity occur in July (15.8 °C and 9.1 g kg<sup>-1</sup>, respectively) and the minima of precipitation occur in August (39.6 mm). The monthly mean maximum of air temperature and specific humidity occur in February (22.4 °C and 14.6 g kg<sup>-1</sup>, respectively) and the maxima of precipitation is observed in January (237 mm) (Sánchez et al., 2019).

Large-scale air circulation in the MRSP is controlled by the position and intensity of the semi-permanent south Atlantic subtropical high and continental low-pressure systems, which induce weak surface winds from north to northeast during the summer and from northeast to east in winter (Oliveira et al., 2003). The minima wind intensity occurs in May (2.3 m s<sup>-1</sup>) and the maxima in November (3.1 m s<sup>-1</sup>) (Sánchez et al. 2019). The large-scale pattern is often disturbed by the passage of cold fronts throughout the year, with a higher frequency in the winter. Cold fronts induce pre-frontal northwest winds and post-frontal southeast winds. In addition to these systems, the MRSP is influenced by three local circulations: the sea breeze, the mountain-valley circulation and the UHI (Ribeiro et al., 2018). These thermally induced flows are the result of the distance to the ocean, topographical configuration and the increase of urbanization.

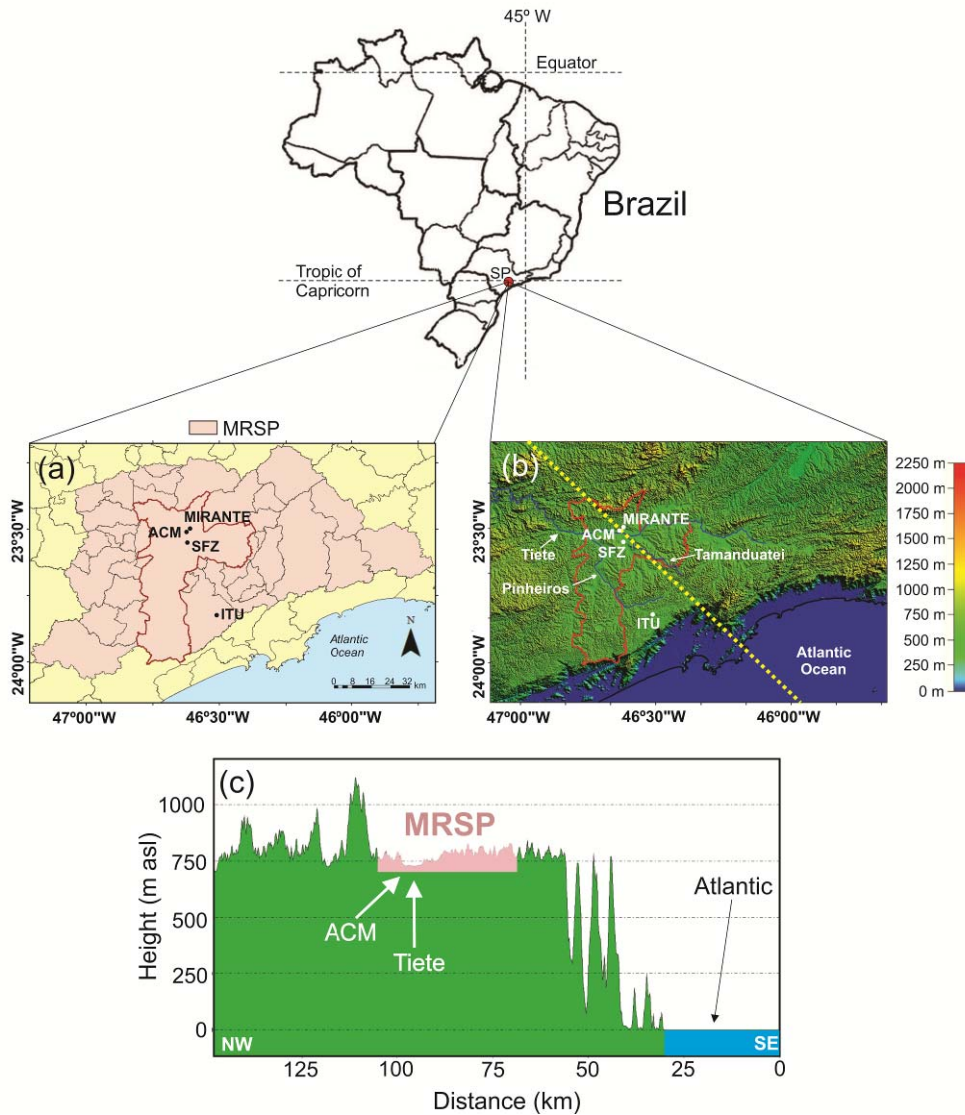


**Fig. 1.** Geographic features of the MRSP. The city of São Paulo is indicated by red borders. All the remaining 38 cities are also indicated. The observation sites are indicated by SFZ (“Secretaria da Fazenda”), ITU (“Itutinga”), ACM (“Campo de Marte” Airport) and MIRANTE (“Mirante de Santana”). Topography is based on the highest-resolution topographic data (3-arc-second Resolution - 90 m), available at <https://www2.jpl.nasa.gov/srtm/>. The dashed yellow line indicates a cross section in the northwest-southeast direction in (b), which is shown in (c).

## 2.2. Measurements and data

This work is based on 160 radio soundings carried out at the ACM (23°30'32" S, 46°38'04" W, 722 m, Fig. 1) as part of the field campaigns of the MCITY BRAZIL Project. The vertical profiles of wind speed and direction, relative humidity and air temperature were obtained using a DIGORA III data acquisition system and radiosonde model RS92-GSP, manufactured by Vaisala, Inc. A description of the equipment characteristics and accuracy of measurements can be found in Sánchez et al. (2019).

The radio soundings were released with a frequency of 3 hours during two periods of 10 consecutive days, in the summer (February 19 to March 1, 2013) and winter (August 6 to 16, 2013) field campaigns (Oliveira et al., 2019). The vertical resolution of radio soundings (vertical distance between two consecutive points from surface to 4000 m) prevailed between 61-70 m and the measurements can be considered representative of the urban area of MRSP because the balloons at first 4000 m were located within the urban limits (Sánchez et al. 2019).

Radio soundings carried out regularly at ACM twice a day at 0900 LT (1200 GMT) and 2100 LT (0000 GMT) from September 1, 2009 to August 16, 2013 (four years) were used for to describe the seasonal variation of the LLJs in the MRSP. During this period a total of 2600 radio soundings were launched providing vertical profiles of air temperature, relative humidity, wind speed and direction with coarser resolution (301-350 m) than the soundings released during field campaigns of 2013 (Sánchez et al. 2019).

UHI was estimated in the MRSP from near-surface air temperature differences between urban (SFZ micrometeorological platform) and rural area (ITU micrometeorological platform) as:

$$\Delta T = T_{\text{urban}} - T_{\text{rural}} \quad (1)$$

The SFZ micrometeorological platform (23°33'01" S; 46°37'49" W, 741 m asl) comprises a 10-m tower set up in the center of a metallic platform on the top of a 18-story building, 77 m above the ground level (agl) in São Paulo City (Fig. 1a). The ITU micrometeorological platform (23°49'32" S; 46°30'32" W, 760 m asl) consists of a 10-m tower set up at the surface level in a vegetated area in “Itutinga Pilões” State Park located at south of the MRSP (Fig. 1a). Air temperature observations in the SFZ and ITU micrometeorological platforms were continuously carried out with sample frequency of 0.5 Hz at 78.6 m agl and at 1.6 m agl, respectively. A complete description of the sensors and quality control procedure applied to temperature measurements are described in Oliveira et al. (2019).

### 2.3. LLJ definition

In this study the main properties of the LLJs were estimated applying a subjective method based on visual inspection of each vertical profile of wind speed and direction provided by radio soundings carried out in field campaigns of February and August in 2013. This method considers the following conditions: maximum wind speed at the jet nose in the lowest 1000 m above the surface greater or equal to  $2.0 \text{ m s}^{-1}$  and 25 % faster than next minimum. We only considered LLJ event when this local maximum was observed in at least two consecutive soundings (persistence criteria), as indicated in Fig. 2a for the LLJ observed in August 10, 2013 at 0000 LT and 0300 LT. The maximum wind speed ( $V_{LLJ}$ ), wind direction ( $D_{LLJ}$ ) and height ( $Z_{LLJ}$ ) at the LLJ core are estimated for each profile.

Taking into account the different structures that can be observed and the occurrence of multiple maximum in the vertical profile of wind speed, the subjective method allows one to identify the LLJ structure with greater accuracy compared to the different objective methods. Despite the advantages of the subjective method, it is very difficult to apply this method to a very large set of data. For these reasons, we developed an automatic objective method to identify LLJ structures in the radio soundings carried out twice a day during four years between 2009 and 2013. This method considers the same criteria used in the subjective method to identify LLJ during field campaigns of 2013, as indicated in Fig. 2b for sounding carried out in July 24, 2012 at 0900 LT. Due to the time frequency of the regular soundings, it was not possible to apply the persistence criteria used to identify LLJs during field campaigns of 2013.

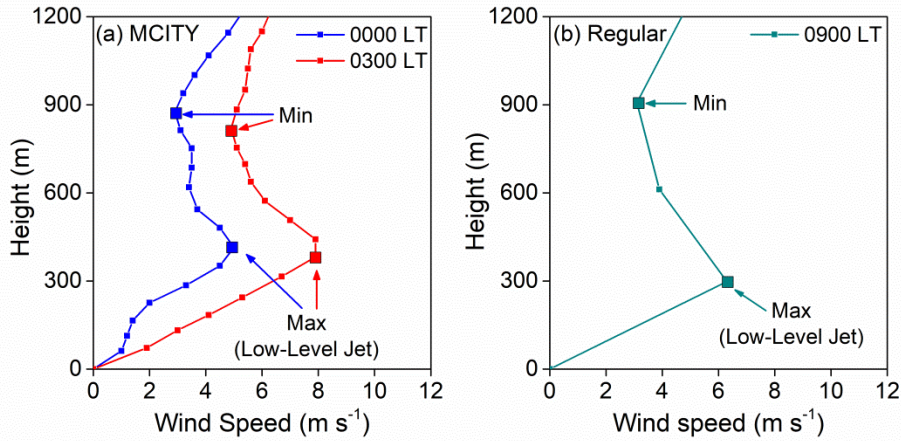


**Fig. 2.** Vertical profiles of wind speed and criteria applied to identify LLJ structure during (a) August 10, 2013 at 0000 LT and 0300 LT (MCITY BRAZIL Project field campaigns) and (b) July 24, 2012 at 0900 LT (regular soundings).

The objective method was previously validated comparing it with the subjective method for two sets of radio soundings with different resolution: field campaigns of February and August of 2013 (finer resolution) (Fig. 3a) and between June and August of 2012 (coarser resolution) (Fig. 3b). The comparison between these two methods was made following three statistical parameters: Mean Bias Error (*MBE*), Root Mean Square Error (*RMSE*) and the Index of Agreement (*d*). The objective method was able to capture the 89 % and 96 % of the LLJ identified through the subjective method during field campaigns of 2013 and between June-August of 2012, respectively. Good agreement was obtained between subjective and objective methods for two set of data (finer and coarser resolution). *MBE*, *RMSE* and *d* are -25 m (-10 m), 149 m (87 m) and 0.89 (0.96) for field campaigns of February and August of 2013 (regular soundings between June-August, 2012). This result indicates that the objective method can be used with good accuracy to identify LLJ structures.

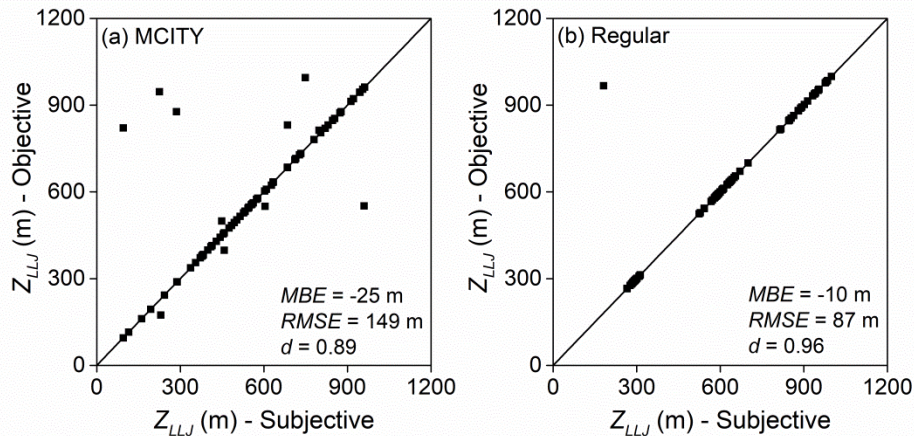


**Fig. 3.** Dispersion diagrams of LLJ heights estimated by subjective and objective method for radio soundings carried out (a) during MCITY BRAZIL Project field campaigns of February and August in 2013 and (b) June, July and August of 2012.

### 3. Results and discussions

#### 3.1. Weather condition effects over the LLJ development

The diurnal evolution of wind speed during two field campaigns in the summer (From 0900 LT on February 19 to 0900 LT on March 1) and in winter (From 0900 LT on August 6 to 0900 LT on August 16) in the first 1500 m of height are indicated in Fig. 4. The dominant synoptic and mesoscale systems on each of the days are represented by symbols in this figure. In general,

LLJs in the MRSP appears in clear-sky conditions with the presence of weak surface winds, as normally occurs during undisturbed conditions and during the influence of high pressure systems.

During the field campaigns of summer, on February 19, 20, 21, 24 and 25 the meteorological patterns in the MRSP were dominated on high level by the influence of upper tropospheric cyclonic vortex, which induced subsidence and favors clear-sky conditions. On the other hand, cloudy conditions were associated with the high-level horizontal divergence due to the combination of the Bolivia high and the upper tropospheric cyclonic vortex circulation (February 26, 27 and 28). Cloudy conditions were also produced by the influence of shortwave upper air troughs (February 22 and 23) and the sea-breeze passage (February 19, 20, 24, 27 and 28) during the afternoon. Sometimes, these systems destabilized the atmosphere and caused an increase in cloudiness, surface winds speed and occurrence of precipitation. Despite the influence of these disturbed systems in few days, the sky remained with little cloudiness for much of the nighttime, which favored the development of the LLJs. These were observed in 9 of 10 nights with soundings (90 %) in summer field campaign. The core of maximum winds associated with the LLJs oscillated between 300 and 900 m and reached the  $10 \text{ m s}^{-1}$  in some nights (Fig. 4a).

During the field campaigns of winter, LLJ events were observed in 8 of 10 nights with soundings (80 %) and are associated with the influence of south Atlantic subtropical high and the post-frontal high pressure systems. From August 6 to 10, prevailing conditions of low cloudiness and weak winds near the surface from north to northeast, which was associated with the major influence of the south Atlantic subtropical high, with its center located on the Atlantic Ocean. These conditions favored the LLJs formation, with maximum intensities varying from 8 to  $13 \text{ m s}^{-1}$  and located between 350 and 700 m (Fig. 4b). On August 10-14, the influence of two cold fronts on the MRSP was observed, and as a consequence there was an increase in the wind speed in the vertical direction and the formation of post-frontal LLJs, with intensity varying from 10 to  $15 \text{ m s}^{-1}$ , between 600 and 1000 m (Fig. 4b). On August 16, the LLJ with maximum intensity of  $13 \text{ m s}^{-1}$  and height of 500 m was observed in the MRSP (Fig. 4b). In general, LLJs associated with cold-fronts passage have a mean intensity and height that is  $3 \text{ m s}^{-1}$  and 329 m greater than LLJs under undisturbed conditions ( $8.4 \pm 0.5 \text{ m s}^{-1}$  and  $436 \pm 31 \text{ m}$ , respectively).

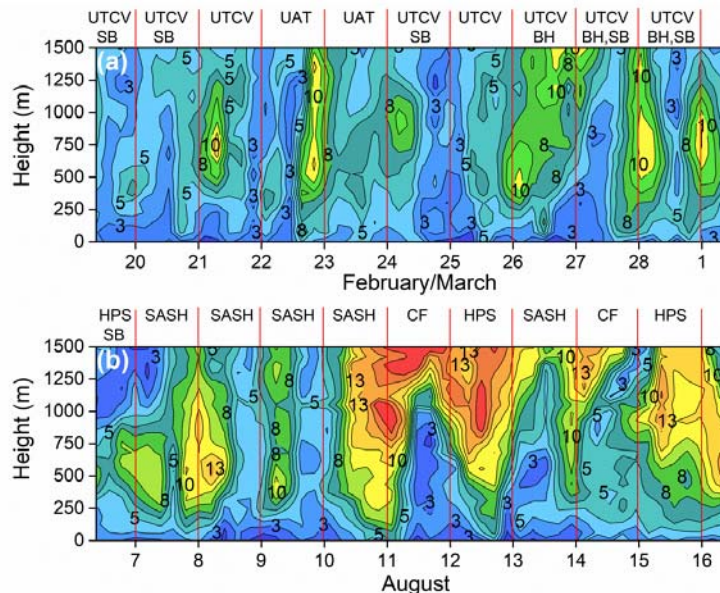


**Fig. 4.** Time evolution of the wind speed up to 1500 m during the field campaigns of (a) February 19 to March 1 and (b) August 6 to 16 in 2013. The symbols correspond to the following synoptic and mesoscale systems: Bolivia High (BH), Upper Tropospheric Cyclonic Vortices (UTCVC), Upper Air Trough (UAT), Sea Breeze (SB), High Pressure System (HPS), South Atlantic Subtropical High (SASH) and Cold Front (CF).

Despite the influence of different synoptic and mesoscale patterns on the development and evolution of LLJs, inertial oscillation seems to be the main mechanism that originates LLJs in the MRSP. Approximately 76 % of the LLJ events (8 in summer and 5 in winter field campaigns) were associated to inertial oscillation (counter-clockwise in Southern Hemisphere). Figure 5 presents the wind hodographs based on radio soundings data linearly interpolated at 200 and 600 m from 1800 LT to 1500 LT for four LLJ events, two in summer (February 23-24 and February 27-28) and two in winter (August 6-7 and August 14-15) in 2013, in which a clear inertial oscillation is seen. At the height of 200 m, a counter-clockwise wind rotation related to the inertial oscillation can be observed, which is best represented at 600 m. Similar results were obtained by Barlow et al. (2015) in London, UK, using Lidar. According to Barlow et al. (2015), in urban areas the inertial oscillation is most clear above the LLJ maximum and it can be interrupted near the surface due to the increase of the roughness and the surface heating. Results obtained by Baas et al. (2009) showed that inertial oscillation is also the main mechanism of LLJs formation in Cabauw, Netherlands.

It is important to note that this idealized development of the LLJs due to the mechanism of inertial oscillation is not always observed, since on occasions the decoupling of the air above the SI layer is not strong enough to generate an inertial oscillation as observed in Fig. 5. In other cases, the presence of mesoscale and synoptic disturbances plays an important role and this idealized behavior will be disturbed.

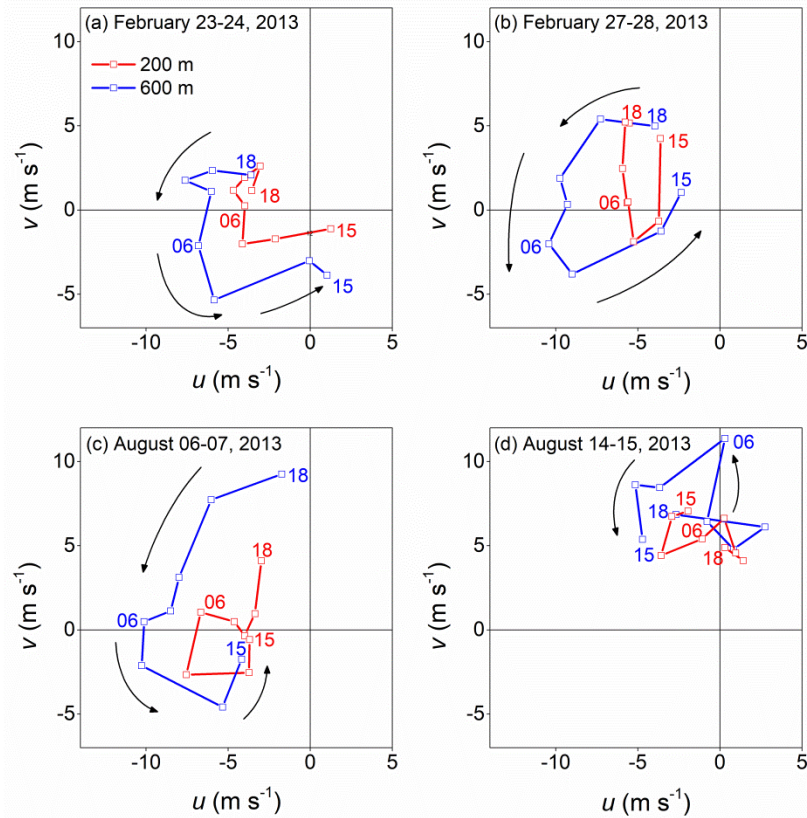


**Fig. 5.** Wind hodographs based on radio sounding data interpolated at 200 and 600 m from 1800 LT to 1500 LT in (a) February 23-24, (b) February 27-28, (c) August 6-7 and (d) August 14-15 in 2013.

### 3.2. LLJ properties

The LLJ structure was observed in 84 soundings during field campaigns in 2013 (47 in February and 37 in August) and in 1652 sounding during 2009-2013. Figure 6 shows the frequency distribution of occurrence, intensity, height, and wind direction associated with LLJs during two fields campaigns of MCITY BRAZIL Project in 2013 (radio soundings with finer resolution) and between 2009 and 2013 (regular radio soundings with coarse resolution) in the MRSP. The



LLJs occurs most frequently between 2100 LT and 0900 LT (80 % of LLJ soundings) and on most night, LLJs event reaches the maximum intensity between 0300 LT and 0900 LT (82 % of night), indicating that the LLJ in the MRSP can be considered as a nocturnal phenomenon (Fig.6a). With respect to the regular soundings carried out between 2009 and 2013, the LLJ frequency at 0900 LT and 2100 LT was similar (Fig. 6b).

According to the distribution of LLJ intensity, the majority of LLJ ranged between 4 and 12 m s<sup>-1</sup> in two set of soundings analyzed (81 % and 84 % of LLJ soundings during field campaigns in 2013 and between 2009-2013, respectively) (Fig. 6c, d), with an mean intensity of 8.4 ± 0.32 m s<sup>-1</sup> during the field campaigns in 2013 and of 7.8 ± 0.07 m s<sup>-1</sup> from 2009 to 2013.

The LLJ height distributions shows that the LLJs varied from 95 m to 962 m during field campaigns in 2013, with the largest number of LLJ cases in the height class of 500-600 m and the mean LLJ height was 541 ± 26 m (Fig. 6e). In the period of regular soundings between 2009 and 2013, the LLJ height showed a trimodal behavior, which is associated with the coarser vertical resolution of the soundings (301-350 m). The most frequent height class was also 500-600 m and mean LLJ height was 640 ± 5 m (Fig. 6f). These results show that the LLJ in the MRSP has similar properties (height and intensity) to the LLJ observed in other regions, such as in North Florida, USA (Karipot et al., 2009); Central Western Mexico (Arfeuille et al., 2015); Moscow, Russia (Kallistratova and Kouznetsov, 2012); Yangtze River Delta, China (Wei et al., 2013) and Cabauw, Netherlands (Baas et al., 2009).

Figure 6g, h shows the wind direction in the core of the LLJ during field campaigns in 2013 and during the period of regular soundings between 2009 and 2013, respectively. In both periods, the predominant direction was from east (31 % and 26 % of LLJ soundings). Other predominant LLJ directions during field campaigns were north (25 %), northeast (18 %), northwest (11 %) and southeast (10 %). During the four years of regular soundings, southeast (20 %), north (13 %), northwest (12.5 %) and northeast (12 %) also predominated. The LLJs from south, west and southwest directions had a lower occurrence in both periods of sondagens. This behavior indicates that LLJ with east, northeast and north direction may be associated with a greater influence of south Atlantic subtropical high and modulated by topography. South and southeast LLJ can be generated under the influence of a synoptic pattern dominated by the post-frontal high pressure system. The inspection of synoptic map (not shown) indicates that 24 % of LLJ events are post-frontal. Some LLJ of east and southeast direction observed at 1500 LT and 1800 LT can be caused by the sea-breeze passage in the afternoon, which is generated by the differential heating between the continent and the sea surface of the Atlantic Ocean and intensified by the topography (“Serra do Mar”) and the interaction with the UHI circulation in the urban area of the MRSP (Ribeiro et al., 2018).

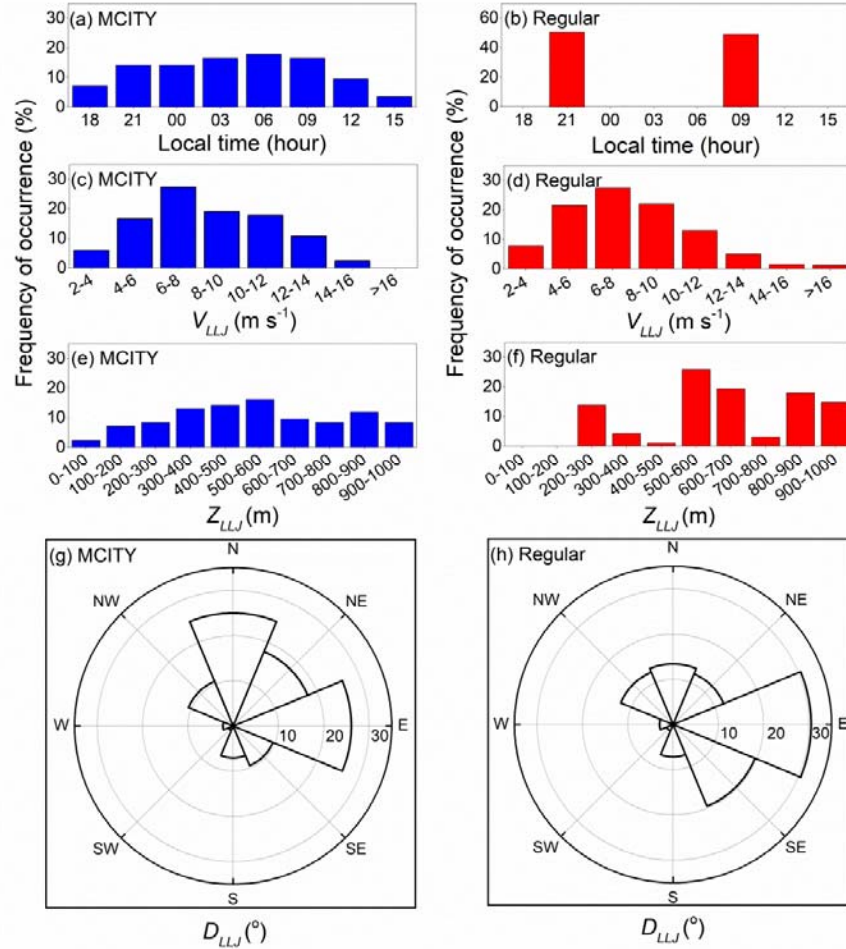


**Fig. 6.** LLJ properties in the MRSP during (a-c-e-g) summer and winter fields campaigns of 2013 based on the subjective method and (b-d-f-h) regular soundings carried out between 2009-2013 based on objective method. Histograms of (a)-(b) LLJ occurrence, (c)-(d) LLJ wind speed, (e)-(f) LLJ height and (g)-(h) LLJ direction.

### 3.3. Interaction between LLJ, UHI and SI layer

According to Oliveira et al. (2019) the UHI intensity in MRSP is weak during daytime and reaches a minimum between 0900 and 1300 LT, it increased considerably around the evening transition and reached a maximum value at approximately midnight and depending on the months of the year another maximum is observed during the afternoon.

The relationship between mean nocturnal UHI intensity, LLJ speed and SI layer strength in the MRSP during August 6-16, 2013 is illustrated in Fig. 7. The SI layer strength was estimated from radio soundings data by  $\Delta\theta_{SI}/Z_{SI}$ , where  $\Delta\theta_{SI} = \theta(Z_{SI}) - \theta_0$ ,  $Z_{SI}$  is the height of the SI layer top and  $\theta_0$  is the potential temperatures at the surface. It is observed that LLJ speed and UHI intensity are negatively correlated according to Pearson correlation coefficient ( $r = -0.80$ ), that is, during the presence of strong LLJ, the UHI intensity was smaller and during episode of weak LLJ, the mean nocturnal UHI intensity reached high values (Fig. 7a, b). A negative correlation was also observed between mean values of LLJ speed and SI layer intensity ( $r = -0.75$ ) (Fig. 7e, f). It indicates that the LLJ generates a turbulent downward flow due to wind shear below the LLJ core, which increases the vertical mixing and limits the development of thermal SI layer. This process was schematically represented and verified by Kutscher et al. (2012) from a comparison of the vertical profile of potential temperature and wind speed between cases with and without LLJ during sounding campaign of summer 2005 in the Negev desert of Israel. On the other hand, the LLJ transport the cold air from rural areas to the urban areas, which is mixed

with hot air when it reaches the city due to the vertical shear generated by the LLJ. It contributes to decrease the UHI intensity. After LLJ passing through the city, the hot air transported by the LLJ is mixed with the cold air of the adjacent rural area and as consequence the UHI effect is horizontally expanded. This behavior suggests that LLJ played an important role in modulating the UHI intensity in MRSP, as previously verified by Hu et al. (2013a) in Oklahoma, USA during July 2003. It was also observed that in the presence of abundant cloud associated with synoptic disturbances, such as cold-fronts passage on August 11 and 14 by the MRSP, the development of LLJ and UHI were limited.

Figure 7c show the relationship between mean nocturnal UHI intensity and SI layer strength. It is verified that during nighttime the UHI intensity reached mean nocturnal values higher than 8 °C in some days in which prevailed clear-sky conditions and LLJs weak, favoring the development of the UHI and the SI layer (Fig. 7c). The SI layer strength and UHI intensity are positively correlated ( $r = 0.81$ ) (Fig. 7d). This result implies that thermal SI strength can be used as an indicator for to predict nocturnal UHI intensity, as suggested by Hu et al. (2013a) in Oklahoma, USA.

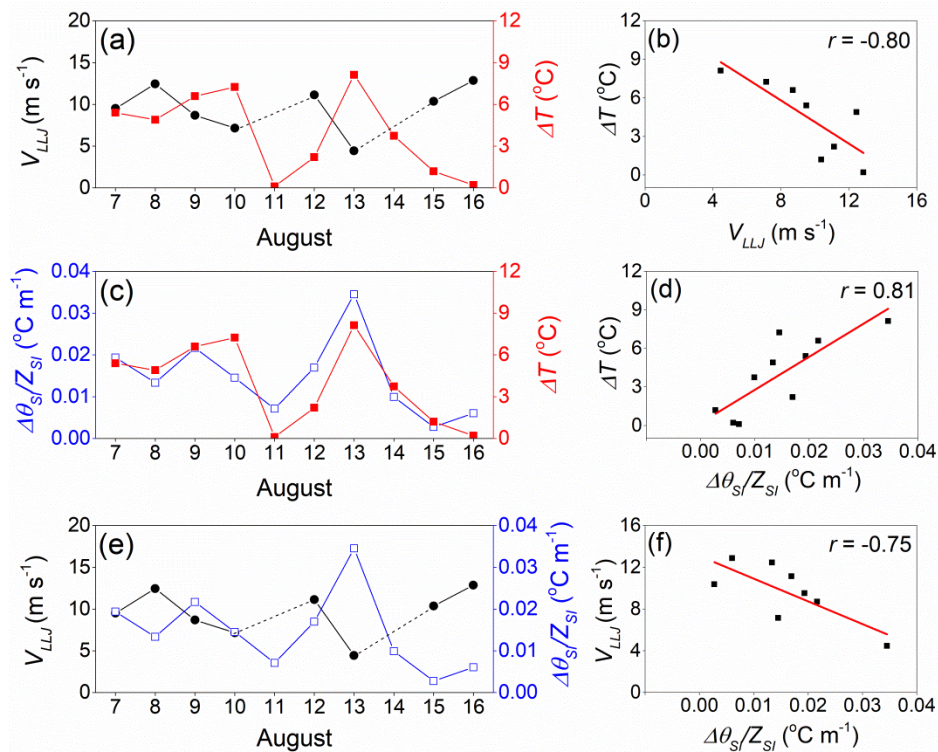


**Fig. 7.** Time evolution and dispersion diagram of mean values during nighttime of (a-b) LLJ speed and nocturnal UHI intensity, (c-d) SI layer strength and nocturnal UHI intensity and (e-f) LLJ speed and SI layer strength in the MRSP during the winter field campaign in 2013. The dashed black lines in (a) and (e) indicate nighttime absence of LLJ.

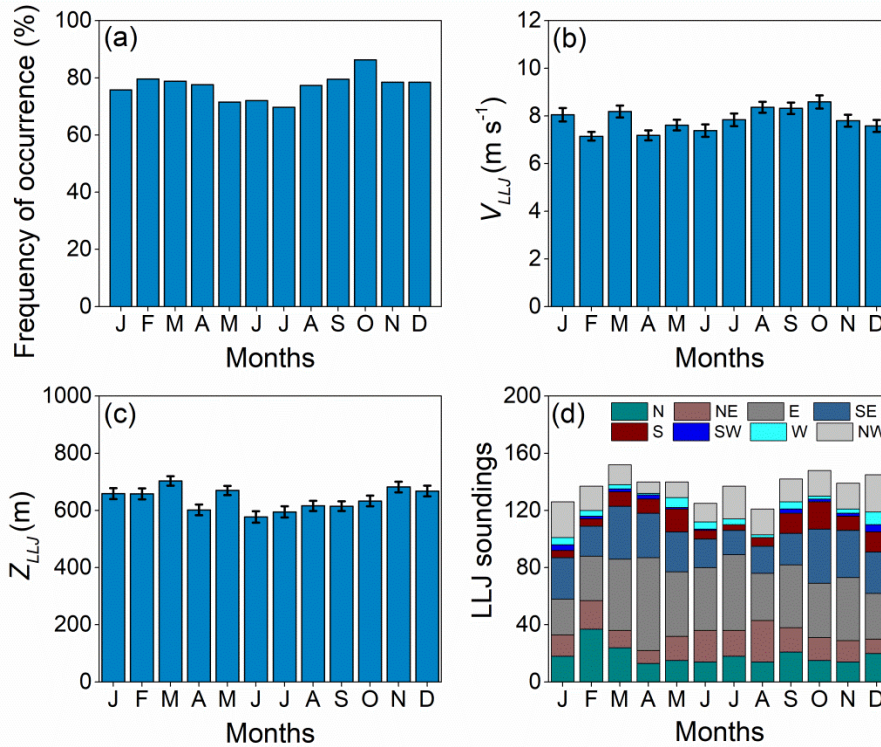
### 3.4. Seasonal variation of LLJ

Figure 8 presents the seasonal distribution of frequency of occurrence, wind direction and monthly mean speed and height of LLJ estimated by the objective method at 0900 LT and 2100 LT during four years between 2009 and 2013. LLJ is very frequent throughout the year, exceeding 65 % of days in all months. From January to April there is a slight increase in the frequency of LLJ occurrence, which appears in more than 75 % of days per months. The occurrence of LLJ decreases from May to cold months of June and July and increases again from August to summer months. The greatest number of days with LLJ was observed in October (86 %) and the least occurrence was observed in July (69 %) (Fig. 8a). According to the frequency of occurrence, the LLJs in the MRSP are as frequent as that observed in Great Plains (Song et al., 2005) and North Florida (Karipot et al., 2009), USA and in the Central Western Mexico (Arfeuille et al., 2015) and is more frequent than the LLJ observed in Cabauw,

Netherlands (Baas et al., 2009) and in the urban areas of Beijing and Guangzhou, China (Miao et al., 2018) and Moscow, Russia (Kallistratova and Kouznetsov, 2012).

Figure 8b, c displays the monthly mean LLJ speed and height, which shows a small seasonal variation. From July to October the LLJ was slightly more intense than the others months, the largest mean value was observed in October ( $8.6 \pm 0.3 \text{ m s}^{-1}$ ) and the smallest was observed in February ( $7.1 \pm 0.2 \text{ m s}^{-1}$ ) (Fig. 8b). With respect to the LLJ height, during summer and autumn months the LLJ occur at slightly higher heights than the ones associated winter and spring months. The higher LLJs were observed in March ( $703 \pm 16 \text{ m}$ ) and the lower LLJs occurred in June ( $577 \pm 20 \text{ m}$ ) (Fig. 8c).

The seasonal variation of wind direction at the core of LLJ indicates that from March to September predominate LLJs from east direction ( $\sim 35\%$  of LLJ soundings). Between October and January an increase in LLJs of south-east direction is observed and in February dominates north LLJs ( $27\%$  LLJ soundings). Another important aspect is that between December and February there is an increase in the occurrence of north and northwest LLJs. This behavior seems to be linked with seasonal variation in the position of the south Atlantic subtropical high and its circulation, the passage of cold front and the influence of local circulation through the MRSP and its interaction with the topography.



**Fig. 8.** Seasonal distribution of (a) frequency of occurrence, (b) mean wind speed, (c) mean height and (d) direction of LLJ events in the MRSP during September 2009-August 2013. The statistical errors are indicated by the vertical bars.

#### 4. Conclusions

The radio soundings carried out during two 10-day field campaigns of the MCITY BRAZIL Project in February and August of 2013 and regular soundings performed regularly at 0900 LT and 2100 LT from September 1, 2009 to August 16, 2013 were used to describe the main features and evolution of LLJs in the MRSP.

The analysis of the vertical profiles of wind speed and direction during field campaigns in 2013 indicated a presence of LLJs in 85 % of the days with soundings, predominantly at nighttime during undisturbed conditions. Most of them were identified between 2100 LT and 0900 LT, reaching maximum intensity at the end of the night and first hours of the morning. The LLJs are mostly in the range of  $4 \leq V_{LLJ} \leq 12 \text{ m s}^{-1}$ ,  $300 \leq Z_{LLJ} \leq 700 \text{ m}$  and  $D_{LLJ}$  from east, north, northeast, southeast and northwest. The hodographs at 200 m and 600 m of height shows that

the inertial oscillation is the main mechanism that originates LLJs in the MRSP. Despite the evidence of the LLJ inertial oscillation, it is not possible to conclude that LLJs in the MRSP are produced only by this mechanism. Baroclinicity induced by land-ocean thermal contrast, topography, urban-rural contrast and synoptic scale disturbances are likely to contribute or even determine this important phenomenon in São Paulo City.

An automatic objective method was applied for to estimate LLJ properties and validated comparing it with the subjective method during field campaigns of 2013 and during June-August of 2012. The comparison indicated that the objective method is well suited to identify LLJ structure and estimate its properties. The seasonal variations of LLJ based on application of the objective method showed that the LLJs are very frequent throughout the year, exceeding 65 % of days in all months. The maximum LLJ occurrence was observed in October (86 % of days) and the minimum frequency occurs in the cold month of July (69 % of days). The LLJ speed and height show a small seasonal variation and prevailed mean intensities less than 10 m s<sup>-1</sup> and mean height between 550-750 m during all months. The predominant monthly wind directions at the maximum wind speed level are east, southeast, north, northeast and northwest. The interactions between LLJ speed, UHI intensity and SI layer strength was assessed during field campaign of August, 2013. The analysis indicate that mechanical mixing associated with LLJs reduces and even eliminates the nocturnal radiative cooling by mixing warmer air from above with cooler air near the surface in the MRSP. The LLJ also plays an important role in reducing the UHI intensity during nighttime in São Paulo City due to the transport of cold air from rural areas to the urban areas by the LLJ. The cold air is mixed with hot air when it reaches the city due to the vertical shear generated by the LLJ, which contributes to decrease the UHI intensity. After LLJ passing through the city, the hot air transported by the LLJ is mixed with the cold air of the rural area and as consequence the UHI effect is horizontally expanded.

## 5. Acknowledgements

This research was sponsored by the Brazilian Research Foundations: FAPESP (2011/50178-5), FAPERJ (E26/111.620/2011 and E-26/103.407/2012), and CNPq (309079/2013-6, 305357/2012-3 and 462734/2014-5). The first author acknowledges the scholarship provided by CNPq. We would like to thank the Brazilian Air Force, especially Brigadier Luiz Cláudio Ribeiro da Silva, Colonel César Augusto Borges Tuna, Lieutenant Colonel Bernardino Simões Neto, Air Force Meteorologists Sergeant Luiz de Oliveira Hirt and Major Milton Osamu Ojumura.

## 6. References

1. Alvares, C. A., Stape, J. L., Sentelhas, P. C., De Moraes Gonçalves, J. L., & Sparovek, G. (2014). Köppen's climate classification map for Brazil. *Meteorologische Zeitschrift*, 22(6), 711–728. <https://doi.org/10.1127/0941-2948/2013/0507>
2. Arfeuille, G., Quintanilla-Montoya, A. L., González, F. C. V., & Villarreal, L. Z. (2015). Observational characteristics of low-level jets in central western Mexico. *Boundary-Layer Meteorology*, 155, 483–500. <https://doi.org/10.1007/s10546-015-0005-0>
3. Baas, P., Bosveld, F. C., Baltink, H. K., & Holtslag, A. A. M. (2009). A climatology of nocturnal low-level jets at Cabauw. *Journal of Applied Meteorology and Climatology*, 48(8), 1627–1642. <https://doi.org/10.1175/2009JAMC1965.1>
4. Barlow, J. F. (2014). Progress in observing and modelling the urban boundary layer. *Urban Climate*, 10, 216–240. <https://doi.org/10.1016/j.uclim.2014.03.011>
5. Barlow, J. F., Halios, C. H., Lane, S. E., & Wood, C. R. (2015). Observations of urban boundary layer structure during a strong urban heat island event. *Environmental Fluid Mechanics*, 15, 373–398. <https://doi.org/10.1007/s10652-014-9335-6>
6. Blackadar, A. K. (1957). Boundary layer wind maxima and their significance for the growth of nocturnal inversions. *Bulletin of the American Meteorological Society*. <https://doi.org/10.1175/1520-0477-38.5.283>
7. Du, Y., Qinghong, Z., Chen, Y.-L., Zhao, Y., & Wang, X. (2014). Numerical simulations of

- spatial distributions and diurnal variations of low-level jets in China during early summer. *Journal of Climate*, 27(2010), 5747–5767. <https://doi.org/10.1175/JCLI-D-13-00571.1>
8. Holton, J. R. (1967). The diurnal boundary layer wind oscillation above sloping terrain. *Tellus*, 19, 199–205. <https://doi.org/10.3402/tellusa.v19i2.9766>
  9. Hu, X.-M., Klein, P. M., Xue, M., Lundquist, J. K., Zhang, F., & Qi, Y. (2013). Impact of low-level jets on the nocturnal urban heat island intensity in Oklahoma City. *Journal of Applied Meteorology and Climatology*, 52, 1779–1802. <https://doi.org/10.1175/JAMC-D-12-0256.1>
  10. Hu, X., Klein, P. M., Xue, M., Zhang, F., Doughty, D. C., Forkel, R., et al. (2013). Impact of the vertical mixing induced by low-level jets on boundary layer ozone concentration. *Atmospheric Environment*, 70, 123–130. <https://doi.org/10.1016/j.atmosenv.2012.12.046>
  11. IBGE (2018). IBGE Demographics Censuses (available at <https://cidades.ibge.gov.br/>, accessed on October 2019)
  12. Jones, C. (2019). Recent changes in the South America low-level jet. *Npj Climate and Atmospheric Science*, 2(1), 1–8. <https://doi.org/10.1038/s41612-019-0077-5>
  13. Kallistratova, M., Kouznetsov, R. D., Kuznetsov, D., Kuznetsova, I. N., Nakhaev, M., & Chirokova, G. (2009). Summertime low-level jet characteristics measured by sodars over rural and urban areas. *Meteorologische Zeitschrift*, 18(3), 289–295. <https://doi.org/10.1127/0941-2948/2009/0380>
  14. Kallistratova, M. A., & Kouznetsov, R. D. (2012). Low-level jets in the Moscow region in summer and winter observed with a Sodar network. *Boundary-Layer Meteorology*, 143, 159–175. <https://doi.org/10.1007/s10546-011-9639-8>
  15. Karam, H. A. (2002). *Estudo do Jato de Baixos Níveis de Iperó e das Implicações no Transporte de Poluentes no Estado de São Paulo*. Universidade de São Paulo.
  16. Karipot, A., Leclerc, M. Y., & Zhang, G. (2009). Characteristics of nocturnal low-level jets observed in the north Florida area. *Monthly Weather Review*, 137, 2605–2621. <https://doi.org/10.1175/2009MWR2705.1>
  17. King, J. C., Lachlan-Cope, T. A., Ladkin, R. S., & Weiss, A. (2008). Airborne measurements in the stable boundary layer over the Larsen Ice Shelf, Antarctica. *Boundary-Layer Meteorology*, 127(3), 413–428. <https://doi.org/10.1007/s10546-008-9271-4>
  18. Klein, P. M., Hu, X. M., & Xue, M. (2014). Impacts of mixing processes in nocturnal atmospheric boundary layer on urban ozone concentrations. *Boundary-Layer Meteorology*, 150(1), 107–130. <https://doi.org/10.1007/s10546-013-9864-4>
  19. Klein, P. M., Hu, X., Shapiro, A., & Xue, M. (2016). Linkages between boundary-layer structure and the development of nocturnal low-level jets in central Oklahoma. *Boundary-Layer Meteorology*, 158(3), 383–408. <https://doi.org/10.1007/s10546-015-0097-6>
  20. Kutsher, J., Haikin, N., Sharon, A., & Heifetz, E. (2012). On the formation of an elevated nocturnal inversion layer in the presence of a low-level jet: A case study. *Boundary-Layer Meteorology*, 144, 441–449. <https://doi.org/10.1007/s10546-012-9720-y>
  21. Li, D., Storch, H. Von, Yin, B., Xu, Z., Qi, J., Wei, W., & Guo, D. (2018). Low-level jets over the Bohai Sea and Yellow Sea: Climatology, variability, and the relationship with regional atmospheric circulations. *Journal of Geophysical Research: Atmospheres*, 123, 5240–5260. <https://doi.org/10.1029/2017JD027949>
  22. Li, J., & Chen, Y.-L. (1998). Barrier jets during TAMEX. *Monthly Weather Review*, 126, 959–971. [https://doi.org/10.1175/1520-0493\(1998\)126<0959:BJDT>2.0.CO;2](https://doi.org/10.1175/1520-0493(1998)126<0959:BJDT>2.0.CO;2)
  23. Lundquist, J. K. (2003). Intermittent and elliptical inertial oscillations in the atmospheric boundary layer. *Journal of the Atmospheric Sciences*, 60(21), 2661–2673. [https://doi.org/10.1175/1520-0469\(2003\)060<2661:iaei>2.0.co;2](https://doi.org/10.1175/1520-0469(2003)060<2661:iaei>2.0.co;2)
  24. Marengo, J. A., Soares, W. R., Saulo, C., & Nicolini, M. (2004). Climatology of the low-level jet east of the Andes as derived from the NCEP – NCAR reanalyses: Characteristics and temporal variability. *Journal of Climate*, 17, 2261–2280.
  25. Miao, Y., Guo, J., Liu, S., Wei, W., Zhang, G., Lin, Y., & Zhai, P. (2018). The climatology of low-level jet in Beijing and Guangzhou, China. *Journal of Geophysical Research: Atmospheres*, 123, 2816–2830. <https://doi.org/10.1002/2017JD027321>

26. Montini, T. L., Jones, C., & Carvalho, L. M. V. (2019). The South American low-level jet: A new climatology, variability, and changes. *Journal of Geophysical Research: Atmospheres*, *124*, 1200–1218. <https://doi.org/10.1029/2018JD029634>
27. Oliveira, A. P., Bornstein, R. D., & Soares, J. (2003). Annual and diurnal wind patterns in the city of São Paulo. *Water, Air, and Soil Pollution: Focus*, *3*, 3–15. <https://doi.org/10.1023/A:1026090103764>
28. Oliveira, Amauri P., Marques Filho, E. P., Ferreira, M. J., Codato, G., Ribeiro, F. N. D., Landulfo, E., et al. (2019). Assessing urban effects on the climate of metropolitan regions of Brazil - Implementation and preliminary results of the MCITY BRAZIL project. (Under revision at the *Theoretical and Applied Climatology*).
29. Parish, T. R. (1982). Barrier winds along the Sierra Nevada mountains. *Journal of Applied Meteorology*, *21*, 925–930.
30. Parish, T. R. (2000). Forcing of the summertime low-level jet along the California coast. *Journal of Applied Meteorology*, *39*(12 PART 2), 2421–2433. [https://doi.org/10.1175/1520-0450\(2000\)039<2421:FOTSLL>2.0.CO;2](https://doi.org/10.1175/1520-0450(2000)039<2421:FOTSLL>2.0.CO;2)
31. Parish, Thomas R. (2017). On the forcing of the summertime Great Plains low-level jet. *Journal of the Atmospheric Sciences*, *74*(12), 3937–3953. <https://doi.org/10.1175/JAS-D-17-0059.1>
32. Ribeiro, F. N. D., Oliveira, A. P., Soares, J., Miranda, R. M., Barlage, M., & Chen, F. (2018). Effect of sea breeze propagation on the urban boundary layer of the metropolitan region of São Paulo, Brazil. *Atmospheric Research*, *214*, 174–188. <https://doi.org/10.1016/j.atmosres.2018.07.015>
33. Sánchez, M. P., Oliveira, A. P., Varona, R. P., Tito, J. V., Codato, G., Ribeiro, F. N. D., et al. (2019). Radiosonde based analysis of the urban boundary layer in the metropolitan region of São Paulo, Brazil. (Under revision at the *Earth and Space Science*).
34. Shapiro, A., Fedorovich, E., & Rahimi, S. (2016). A unified theory for the Great Plains nocturnal low-level jet. *Journal of the Atmospheric Sciences*, *73*, 3037–3057. <https://doi.org/10.1175/JAS-D-15-0307.1>
35. Song, J., Liao, K., Coulter, R. L., & Lesht, B. M. (2005). Climatology of the low-level jet at the southern Great Plains Atmospheric Boundary Layer Experiments site. *Journal of Applied Meteorology*, *44*, 1593–1606.
36. Stull, R. B. (1988). *An introduction to boundary layer meteorology*. Kluwer Academic Publishers, Dordrecht.
37. Sullivan, J. T., Rabenhorst, S. D., Dreessen, J., Mcgee, T. J., Delgado, R., Twigg, L., & Sumnicht, G. (2017). Lidar observations revealing transport of O<sub>3</sub> in the presence of a nocturnal low-level jet: Regional implications for “next-day” pollution. *Atmospheric Environment*, *158*, 160–171. <https://doi.org/10.1016/j.atmosenv.2017.03.039>
38. Wang, Y., Klipp, C. L., Garvey, D. M., Ligon, D. A., Williamson, C. C., Chang, S. S., et al. (2007). Nocturnal low-level-jet-dominated atmospheric boundary layer observed by a Doppler lidar over Oklahoma City during JU2003. *Journal of Applied Meteorology and Climatology*, *46*, 2098–2109. <https://doi.org/10.1175/2006JAMC1283.1>
39. Wei, W., Wu, B. G., Ye, X. X., Wang, H. X., & Zhang, H. S. (2013). Characteristics and mechanisms of low-level jets in the Yangtze River Delta of China. *Boundary-Layer Meteorology*, *149*, 403–424. <https://doi.org/10.1007/s10546-013-9852-8>
40. Whiteman, C. D., Bian, X., & Zhong, S. (1997). Low-level jet climatology from enhanced rawinsonde observations at a site in the southern Great Plains. *Journal of Applied Meteorology*, *36*, 1363–1376.
41. Van de Wiel, B. J. H., Moene, A. F., Steeneveld, G. J., Baas, P., Bolveld, F. C., & Holtslag, A. A. M. (2010). A conceptual view on inertial oscillations and nocturnal low-level jets. *Journal of the Atmospheric Sciences*, *67*, 2679–2689. <https://doi.org/10.1175/2010JAS3289.1>
42. Zhang, Y., Xue, M., Zhu, K., & Zhou, B. (2019). What is the main cause of diurnal variation and nocturnal peak of summer precipitation in Sichuan Basin, China? The key role of boundary layer low-level jet inertial oscillations. *Journal of Geophysical Research: Atmospheres*, *124*, 2643–2664. <https://doi.org/10.1029/2018JD029834>